JOURNAL OF SPACECRAFT AND ROCKETS
Vol. 31, No. 6, November-December 1994

Wing Vertical Position Effects on Wing–Body Carryover for Noncircular Missiles

Brian E. Est* and H. F. Nelson†
University of Missouri—Rolla, Rolla, Missouri 65401

The preliminary design component buildup factor $K_{W(B)}$, a measure of the wing–body interference caused by upwash, is investigated for unbanked, supersonic missiles with noncircular body cross section. The aerodynamic effects of wing vertical location relative to the missile fuselage centerline, Mach number, and fuselage cross-sectional shape are parametrically varied to develop a preliminary design data base of $K_{W(B)}$ values for circular, square, and triangular missile bodies. A spatial marching Euler code ZEUS is used to determine the delta-wing normal force in the presence of the body. Euler $K_{W(B)}$ predictions are compared to the slender body theory presently used for computing low angle-of-attack $K_{W(B)}$ in missile preliminary design engineering methods. Euler values of $K_{W(B)}$ exhibit sensitivity to wing vertical position, Mach number, and body cross-sectional shape, whereas slender body theory is a function of wing semispan to body radius ratios, S/R, only. Euler values of $K_{W(B)}$ are generally found to differ from slender body theory values by less than 15% for smaller S/R, and they approach slender body theory values at larger S/R.

Nomenclature

a = shape parameter
C_N = normal force coefficient
C_{N_α} = normal force curve slope, deg^{-1}
C_P = pressure coefficient
H = wing vertical position from longitudinal body axis, cm
$K_{W(B)}$ = carryover on wing due to presence of the body
$k_{W(B)}$ = interference caused by all-moving control deflection
M = Mach number
r = radial direction from missile centerline, cm
R = radius of inscribed circle in missile base, cm
R_f = radius of circular fillet (see Fig. 14)
S = wing semispan from body centerline, cm
V = freestream velocity, m/s
V_c = crossflow velocity, $V \sin \alpha$, m/s
V_{NW} = component of crossflow velocity normal to wing, m/s
V_t = component of crossflow velocity tangent at body surface, m/s
y = lateral position from missile centerline, cm
Z = axial position from nose tip, cm
α_C = missile angle of attack, deg
α_W = wing angle of attack, deg = $\alpha_C \cos \phi$
β_W = wing sideslip angle, deg = $\alpha_C \sin \phi$
δ_W = all-moving control surface deflection angle, deg
$\Delta\alpha_v$ = incremental angle of attack caused by flowfield vortices, deg
ϕ = aerodynamic roll angle or angular position in crossflow plane, deg
Λ = wing leading-edge sweep back angle, 51.34 deg
Θ = included angle between V_t and V_{NW}, deg

Subscripts
W = wing alone
$W(B)$ = wing in presence of body

Introduction

Background

MANY shipborne and landborne tactical missile systems are stored, transported, and fired from armored box launch containers. Many airborne tactical missile systems are required to be stored in internal bomb bays or in conformal carriage configurations for stealth and low drag considerations. Common to all launch container systems is that the missiles are packaged in containers of various geometric cross-sectional shapes to facilitate compact unit storage and efficient reload capability, as illustrated in Fig. 1. The fuselage cross section of most missiles is circular and does not efficiently utilize the volume of the noncircular launch container. Shipborne and landborne missiles with a fuselage cross-sectional shape more like the noncircular launch container would contain more internal volume available for fuel, warhead/submunitions, and

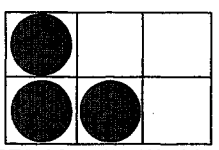

ARMORED BOX LAUNCH CONTAINER
SQUARE CROSS SECTION

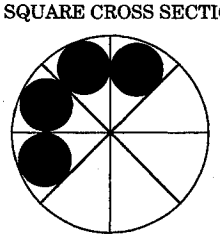

ROTARY LAUNCH CONTAINER
TRIANGULAR CROSS SECTION

Fig. 1 Cross-sectional shapes of several types of missile launch containers.

Presented as Paper 92-0078 at the AIAA 30th Aerospace Sciences Meeting, Reno, NV, Jan. 6–9, 1992; received Jan. 30, 1992; revision received May 18, 1993; accepted for publication Sept. 14, 1993.

*Graduate student, Department of Mechanical and Aerospace Engineering and Engineering Mechanics; currently Aerospace Engineer, Dynetics, Inc., Flight Vehicle Analysis Branch, 1000 Explorer Blvd., Huntsville, AL 35814-5050. Member AIAA.

†Professor Aerospace Engineering, Thermal Radiative Transfer Group. Associate Fellow AIAA.

seeker. Airborne missiles with a flat windward or leeward facet (triangular cross section) would be advantageous for conformal carriage or for internal rotary launcher systems.

A primary design factor for all missiles stored inside a launch container is wing packaging prior to ejection. Wings that cannot be recessed inside the missile fuselage cavity must be folded externally around the body moldline. In some instances, rigid, planar wings with semispans large in relation to the fuselage cross-sectional radius cannot be folded circumferentially around the fuselage because of geometric and structural constraints. However, horizontal wing root-chord locations, H/R, vertically above ($+H/R$) and below ($-H/R$) the missile centerline allow the designer flexibility in wing semispan selection, as illustrated in Fig. 2. Horizontal wing positions above and below the missile centerline were considered for the noncircular fuselage cross sections of this research.

In addition to larger internal volume, compact packaging, and larger wing semispan, missiles with noncircular fuselage cross sections may offer an attractive stealth characteristic. Previous research has shown that missiles with noncircular fuselage cross sections have increased maneuverability, higher

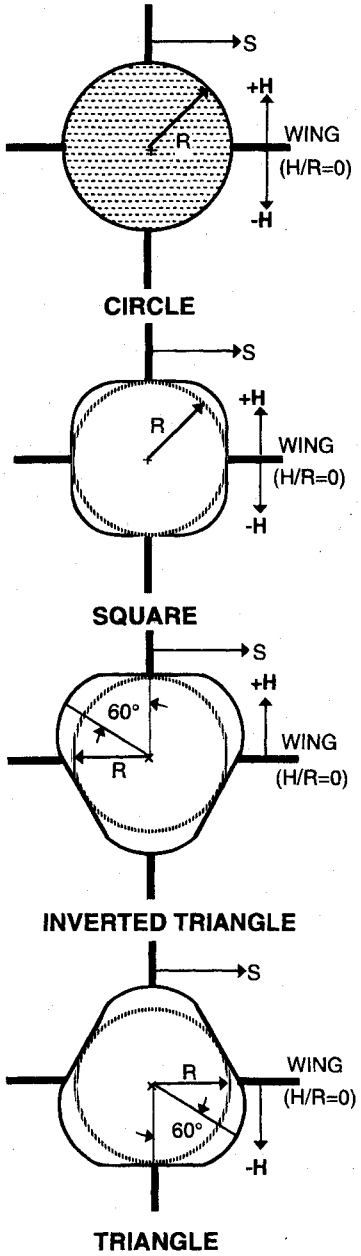

Fig. 2 Fuselage cross-sectional shapes and baseline wing vertical positions ($H/R = 0$).

L/D ratios, and generate larger normal force coefficients than missiles with equivalent circular fuselage cross sections.[1–7]

Aerodynamic Prediction

During conceptual and preliminary tactical missile design, a variety of flight configurations are considered to meet system performance requirements. The configuration design engineer is constrained by time and cost budgets; therefore, methods used to predict the aerodynamic performance of tactical missiles accurately are required to be quick, inexpensive, and easy to apply. Component buildup methods[8–10] have received much attention in missile literature because of their efficiency[11] and accuracy[12,13] of normal force and center of pressure predictions. These component buildup methods have been incorporated into several engineering-level aerodynamic prediction codes; e.g., U.S.A.F. Missile Datcom,[14] Naval Surface Weapons Center Aeroprediction,[15] and Tri-Service Missile III.[16]

One of the most common component build-up techniques is the equivalent angle-of-attack method. This method combines the effects of wing–body carryover and flowfield vortices from the body and lifting surfaces, together with the component-alone normal force curve slope to compute an "equivalent" angle of attack for the wing.[10] The normal force on a wing at low missile angle-of-attack is given by

$$C_{N_{W(B)}} = \alpha_{eq}[C_{N_\alpha}]_W \tag{1}$$

where the equivalent angle of attack at small angles is defined as

$$\alpha_{eq} = K_{W(B)}\alpha_W + K_\phi \alpha_W \beta_W + k_{W(B)}\delta_W + \Delta\alpha_v \tag{2}$$

$K_{W(B)}$, K_ϕ, $k_{W(B)}$, and $\Delta\alpha_v$ correspond to the wing–body carryover caused by the body upwash on an undeflected wing, wing–wing interference caused by sideslip, wing–body interference caused by a control deflection, and flowfield vortex effects, respectively. The wing–body carryover component of the equivalent angle-of-attack method caused by body upwash for an undeflected wing at $\alpha \geq 0$ deg is defined as

$$K_{W(B)} = \frac{(C_{N_\alpha})_{W(B)}}{(C_{N_\alpha})_W} \tag{3}$$

The wing–body carryover contribution to normal force can be nearly twice the magnitude of the wing-alone, therefore, accurate prediction of $K_{W(B)}$ is paramount to the configuration design engineer. Typically, slender body theory (SBT) is used for low angle-of-attack $K_{W(B)}$ predictions used in current aerodynamic prediction codes. $K_{W(B)}$ values from SBT, when used with experimental wing data in the component buildup method, have been shown to yield good agreement with experiment for finned missiles with circular fuselage cross section at low angles of attack.

The objectives of the current effort are: 1) investigate the sensitivity of $K_{W(B)}$ to Mach number, fuselage cross-sectional shape, and wing vertical position relative to the missile centerline; 2) compare Euler $K_{W(B)}$ predictions to slender body theory; and 3) develop a database of $K_{W(B)}$ values suitable for preliminary design of noncircular missiles. Missiles with circular, square, and triangular fuselage cross sections are evaluated at supersonic Mach numbers. The vertical location of the horizontal wings is varied both above and below the body centerline for unbanked, body-wing missiles at low angles of attack.

Analytical Methodology

Governing Equations

The three-dimensional Euler equations are utilized for this research because of their computational efficiency and accuracy of solutions. The pressure distribution given by the Euler equations is accurate for attached, supersonic flow and can be integrated over the entire body to yield normal force, inviscid axial

force, and moment coefficient data. The Euler equations have been shown to give excellent results for missile aerodynamics.[1,5–7] ZEUS,[17–18] a finite volume, spatial marching Euler code based on the upwind Godunov scheme, is used to calculate the wing normal force in the presence of the body data for this investigation.

Est and Nelson[1,5–7] have investigated body-alone and cruciform, body–tail missiles with noncircular fuselage cross section in supersonic cruise. Their results showed good agreement with wind-tunnel data from Carlson and Gapcynski[2] at Mach number = 2, $\alpha \leq 6$ deg, and shape parameters of $a = 0.5122$ and $a = 0.5580$ (see Appendix A) for square and triangular fuselage cross sections, respectively. $K_{W(B)}$ values predicted by ZEUS for cruciform, body–tail missiles in supersonic cruise compared favorably to SBT for square, circular, and triangular cross-sectional shapes for shape $a \leq 0.5$ and $\alpha \leq 5$ deg.

Body Cross-Sectional Shape and Wing Position

All of the fuselage cross-sectional shapes investigated are related by a common shape parameter a. A derivation and illustration of the shape parameter are included in Appendix A. The shape parameter varies from 0 to 1 and it quantifies the fuselage cross-sectional shape. When $a = 0$, all shapes degenerate to a circular cross section with common radius R. When $a = 1.0$, cross-sectional shapes become sharp cornered squares or triangles, depending upon the shape of interest.

The cruciform wings on the missiles are arranged in the "+" attitude ($\phi = 0$ deg). Figure 2 illustrates the baseline wing positions and nomenclature. For the circular and square fuselage cross section, the baseline wing positions are located symmetrically on the body centerline ($H/R = 0$). The horizontal wing position is varied vertically above and below the body centerline ($|H/R| \geq 0$). For the triangular and inverted triangular fuselage cross sections, the baseline horizontal wing position is at the missile centerline and the horizontal wing position is varied toward the shoulder of the triangle. Selection of baseline wing positions was driven by the requirement that the wings be folded while the missile is in the launch container. Placement of the horizontal wings at H/R positions above or below the body centerline enables wings with larger semispans to be utilized.

For the triangular and inverted triangular fuselage cross sections, the wing root-chord is not located at $y/R = 1$, e.g., $y/R = 1.299$ for a wing on an $a = 0.5$ triangular fuselage cross section (see Fig. 2). The wing root-chord y/R position is a function of shape parameter a. This implies that changing the cross-sectional shape of the fuselage (changing the shape parameter) will shift the position of the wing root-chord in relation to the fuselage centerline, resulting in different, shifted values of S/R. For data comparison purposes, it was not practical to account for this shift. Therefore, the position $S/R = 1$ is always located at the wing root-chord independent of the body cross section, and $S/R = 6$ implies a wing with a semispan that extends outwardly five body radii ($5R$) from the wing root-chord.

For the triangular and inverted triangular fuselage cross sections, the calculation of wing vertical position is coupled with the shape parameter. The nominal horizontal fin position is located at the shoulder (center of the circular fillit that comprises the corner) located 60 deg off horizontal for the triangle and inverted triangle. For example, the nominal horizontal wing position for a triangular fuselage cross section with $a = 0.5$ corresponds to a vertical position of $H/R = -0.75$, but for an $a = 0.25$ fuselage cross section, this position corresponds to a vertical position of $H/R = -0.625$ ($a = 0$ corresponds to an $H/R = -0.5$). As the shape parameter increases, the shoulder of the triangles moves outboard and vertically away from the body centerline.

ZEUS Configuration

Figure 3 presents the missile geometry used in this research. The nosecone of the missile is conical and linearly tapers from a circular cross section at $Z/R = 0.3$ to the cross-sectional shape of interest at $Z/R = 6.0$. For $Z/R > 6$, the fuselage has a constant cross-sectional shape. ZEUS computations begin at an initial data plane at $Z/R = 0.3$, generated by a one-dimensional conical starting solution that takes the calculations across the bow shock. The ZEUS calculations are axially marched down the body using a single zone, 36 × 36, (r by ϕ) mesh for the forebody calculations ($0.3 \leq Z/R \leq 35$) at 90% of the CFL step limit. At $Z/R = 35$, the computations are stopped and the code is rezoned for the calculations over the missile wings. ZEUS was configured with two, 36 × 36 zones for $35 < Z/R \leq 43.25$ and run at 20% the CFL limit. For simplicity, mesh clustering was not used, although ZEUS has this capability. By reducing the maximum CFL limit, the computational marching step is reduced; in effect, increasing the number of grid points on the wings to define the flowfield better. Pitch plane symmetry is utilized to reduce computer storage and run time. All of the ZEUS computations were made using the IBM 4381 computer at the University of Missouri—Rolla. CPU times ranged from 66 to 110 min for complete missile flowfield solutions.

Table 1 Nominal flight conditions and wing geometry

Parameter	Range	Nominal value
Mach number, M	2.0, 3.0, 4.0	3.0
Wing leading-edge sweep back angle, Λ	51.34 deg	51.34 deg
Shape parameter, a	$0.0 \leq a \leq 0.5$	0.5
Angle of attack, α	3.0 deg	3.0 deg
Wing vertical position, H/R	$-0.75 \leq H/R \leq 0.75$	0.0

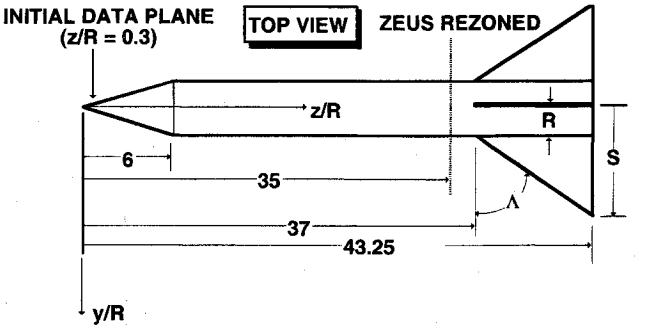

Fig. 3 Missile geometry.

Flight Conditions

The nominal flight conditions for this research are given in Table 1. $K_{W(B)}$ data are presented for a range of flight parametrics, also shown in Table 1.

Wing-Alone Lift

The wings used in this research are zero thickness delta-wings with an unswept trailing edge. The four wings are arranged in a cruciform configuration in the "+" orientation. Supersonic lifting surface theory[9] is used to determine the wing-alone normal force curve slope and is given by

$$(C_{N_\alpha})_W = \frac{4}{\sqrt{M^2 - 1}} \tag{4}$$

This theory is valid for supersonic leading edges and attached flow.

The values of $K_{W(B)}$ presented are related directly to the equation used for the wing-alone normal force slope [see Eq. (3)]. Different methods for calculating the normal force slope would give different values of $K_{W(B)}$. The user can apply the $K_{W(B)}$ results using his or her own normal force prediction

method by multiplying the current $K_{W(B)}$ results by Eq. (4) and dividing by his or her own normal force slope data.

Small S/R Considerations

At small S/R, the prediction of $(C_{N_\alpha})_{W(B)}$ by ZEUS becomes inaccurate because of the small number of grid points located on the wing. In the limit, as S/R approaches 1, the missile becomes a fuselage without wings. Experimental and analytical data exist[20] for cylinders with noncircular cross sections. The analytical data were calculated by using a potential flow conformal mapping transformation of the flow around a two-dimensional noncircular cylinder.

The limiting values of $K_{W(B)}$ as S/R approaches 1 can be calculated from the crossflow velocities over the fuselage. Reference 20 provides pressure coefficient data for the fuselage cross-sectional shapes investigated in this research. For incompressible flow, the velocity is related to the pressure coefficient by

$$\frac{V_t}{V_c} = \sqrt{1 - C_P} \tag{5}$$

where V_c and V_t are the crossflow velocity and tangential surface velocity, respectively. The pressure coefficient yields velocity data that in the limit as S/R approaches 1, is $K_{W(B)}$

$$K_{W(B)} = \frac{V_{NW}}{V_c} \tag{6}$$

where

$$\frac{V_{NW}}{V_c} = \frac{V_t}{V_c}\cos\Theta \tag{7}$$

and Θ is the angle between the velocity tangent to body surface V_t and the velocity normal to the wing planform V_{NW}. From Eqs. (5), (6), and (7)

$$K_{W(B)} = \cos\Theta\sqrt{1 - C_P} \tag{8}$$

In the limit, as S/R approaches 1, the wings vanish and the ZEUS computations should approach the potential flow solutions. Therefore, the ZEUS solutions are extended to match the potential flow solutions at $S/R = 1$. Table 2 contains the potential flow data for $K_{W(B)}$ at $S/R = 1$ for the baseline value of H/R and for $\pm H/R$ displacements from the baseline. These data were linearly interpolated in a to find $K_{W(B)}$ at $S/R = 1$ for the a of interest.

Table 2 $K_{W(B)}$ values as S/R approaches 1

Cross-sectional shape	Limiting value of $K_{W(B)}$ as S/R approaches 1	
Square	$a = 0.00$	$a = 0.60$
$H/R = 0$	2.00	1.50
$\Delta H/R = \pm 0.2$	1.92	1.53
$\Delta H/R = \pm 0.4$	1.68	1.62
Triangle/inverted triangle	$a = 0.00$	$a = 0.65$ (upright/inverted)
$H/R = 0.5/-0.5$	1.50	1.73/1.73
$\Delta H/R = 0.2/-0.2$	1.82	2.04/2.05
$\Delta H/R = 0.4/-0.4$	1.98	1.98/1.75

Results and Discussion

H/R Effects

Wing vertical position effects on $K_{W(B)}$ have been published for missiles with circular fuselage cross sections. Jenn and Nelson[21] used a finite difference code SWINT to predict $K_{W(B)}$ for $-0.9 < H/R < 0.9$. Figure 4 shows the effect of

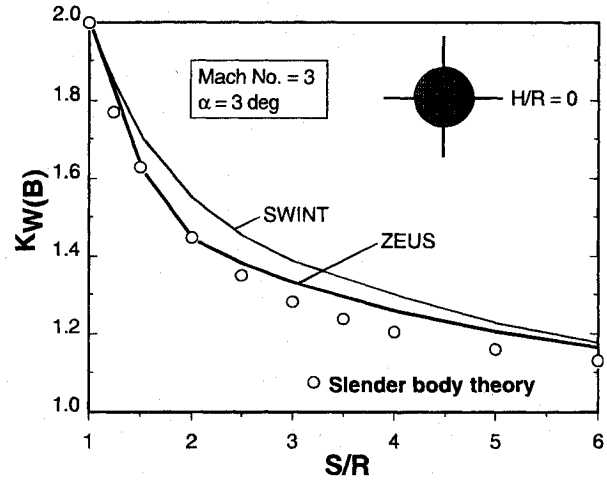

Fig. 4 Comparison of $K_{W(B)}$ predictions by ZEUS, SWINT, and slender body theory as a function of S/R.

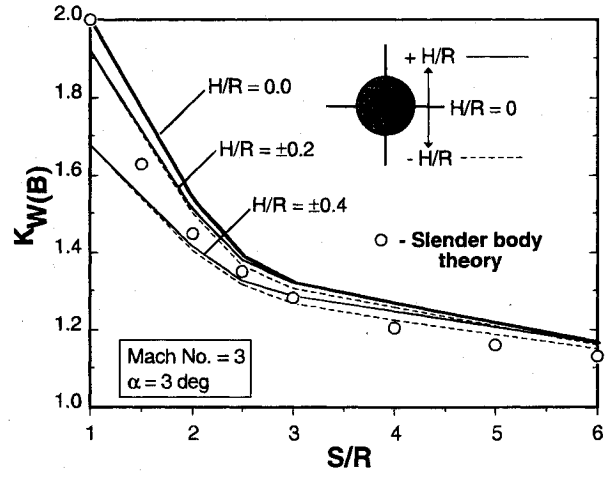

Fig. 5 $K_{W(B)}$ predictions for circular bodies with wings at H/R = 0.0, ± 0.2, and ± 0.4 as a function of S/R.

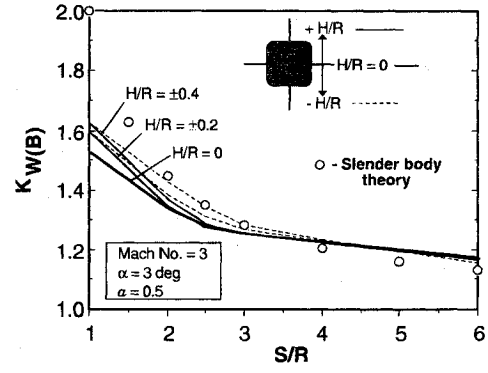

Fig. 6 $K_{W(B)}$ predictions for square bodies with wings at H/R = 0.0, ± 0.2, and ± 0.4 as a function of S/R.

wing semispan on $K_{W(B)}$ for SWINT, ZEUS, and SBT predictions. ZEUS predictions agree closely with SBT as small S/R and approach SWINT values at $S/R \cong 6$.

The effects of wing vertical position above and below the centerline and wing semispan on $K_{W(B)}$ for circular fuselage cross section are shown in Fig. 5. The wing–body interference becomes less favorable as $|H/R|$ increases, i.e., as the wing moves away from the missile centerline. At larger fin semispans, Euler values approach SBT.

The effects of wing vertical position above and below the centerline and wing semispan on $K_{W(B)}$ for $a = 0.5$ square fuselage cross sections are shown in Fig. 6. The effect of moving the wing off the missile centerline is to increase the wing–body interference for $S/R \leq 3$, with downward positions producing the largest $K_{W(B)}$ values. At fin semispans greater than 3, ZEUS predictions approach slender body theory values.

Figure 7 illustrates the effects of positive wing vertical positions and wing semispan on $K_{W(B)}$ for $a = 0.5$ inverted triangular cross sections. $K_{W(B)}$ values become small for H/R positions located near the inverted triangle shoulder at small S/R. At large S/R, $K_{W(B)}$ approaches the same asymptotic value for all wing vertical positions. $K_{W(B)}$ values for H/R positions on the flat side of the fuselage, away from the corner, do not differ appreciably; however, the $K_{W(B)}$ values for the wing located at the corner of the fuselage ($H/R = 0.75$) are considerably lower.

The physical nature of the velocity field around the missile is illustrated in Figs. 8–10 by the crossflow velocity vectors. The arrow length is proportional to the magnitude and it points in the direction of the crossflow velocity. Figures 8 and 9 show an $a = 0.5$ square fuselage cross section with $S/R = 4$ wings located at $H/R = -0.4$ and 0.4, respectively. In Fig. 8, the shock below the wing interacts with the crossflow expanding around the windward fuselage corner. The expansion above the wing interacts with the crossflow expanding around the leeward corner, resulting in a stronger expansion at the leeward corner. In Fig. 9, the wing position above the missile centerline results in a strong expansion around the windward fuselage corner with no interaction with the shock below the wing. The expansion above the wing interacts with the expansion of the crossflow around the leeward corner of the fuselage and results in a reverse flow region above the leeward corner. Figure 10 shows an $a = 0.5$ inverted triangular fuselage cross section with wing $S/R = 5$ located at $H/R = -0.55$. The high-pressure windward flow is captured by the wing, resulting in higher body upwash effects on the horizontal wing.

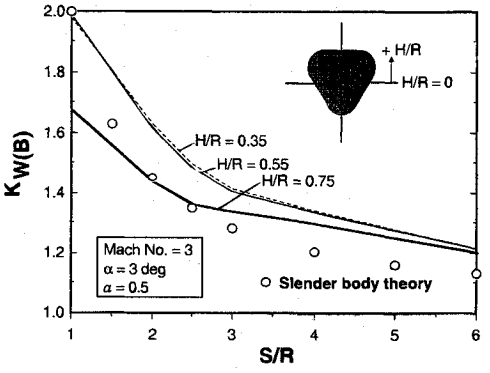

Fig. 7 $K_{W(B)}$ predictions for inverted triangle bodies with wings at $H/R = 0.35$, 0.55, and 0.75 as a function of S/R.

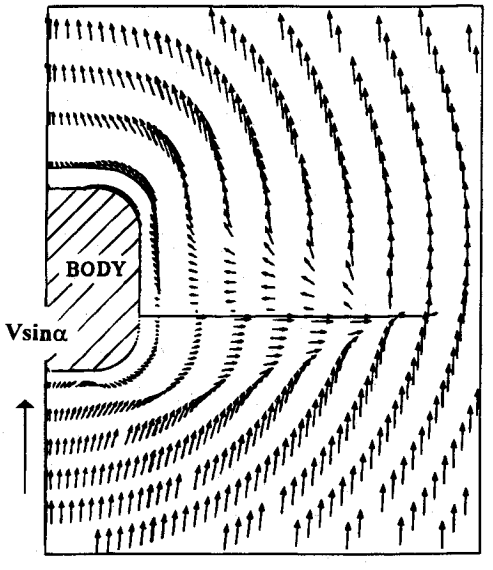

Fig. 8 Crossflow velocity vectors for a square fuselage cross section with $S/R = 4$ wings at $H/R = -0.4$, Mach = 3.0, $\alpha = 3$ deg, and $a = 0.5$.

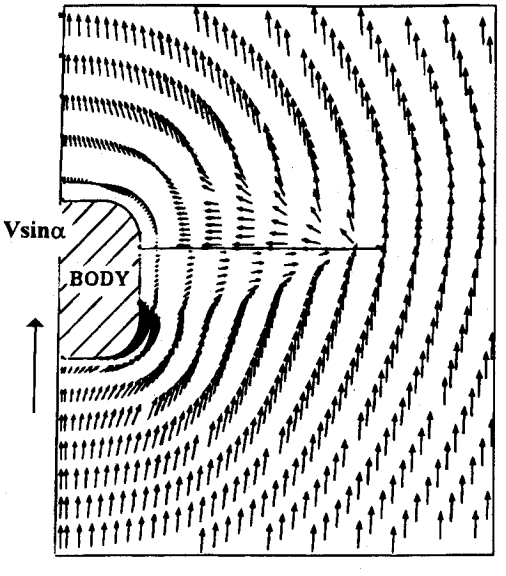

Fig. 9 Crossflow velocity vectors for a square fuselage cross section with $S/R = 4$ wings at $H/R = 0.4$, Mach = 3.0, $\alpha = 3$ deg, and $a = 0.5$.

Body Cross-Sectional Shape Effects

The effects of shape factor and fin semispan on $K_{W(B)}$ for square fuselage cross sections with wings located at $H/R = 0.2$ are illustrated in Fig. 11. Increasing shape parameter decreases the wing–body interference effects for $S/R < 6$. This is attributed to the effect the body has on the crossflow. As the shape parameter increases, the corners of the square fuselage project into the flowfield, effectively maintaining a constant pressure on the windward face of the fuselage. The wing–body interference effects are transported by the crossflow (upwash), and they are strongest near the body and decrease as S/R increases. Therefore, as the crossflow velocity decreases, the magnitude of the favorable wing–body interference reduces correspondingly.

Figure 12 shows that the reverse trend of Fig. 11 is true for the inverted triangular fuselage cross sections with wings located at $H/R = 0.550$, 0.425, and 0.300 for $a = 0.50$, 0.25, and 0.00, respectively (recall H/R is a function of shape parameter). In the inverted triangle case, the wings are coincidental in space although the H/R values are different. As the body cross section becomes increasingly noncircular, the windward corner of the inverted triangle becomes sharper, resulting in larger crossflow

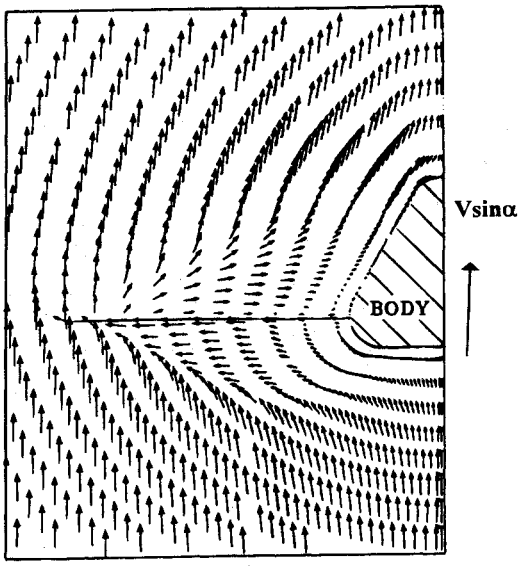

Fig. 10 Crossflow velocity vectors for a triangular fuselage cross section with $S/R = 5$ wings at $H/R = -0.55$, Mach = 3.0, $\alpha = 3$ deg, and $a = 0.5$.

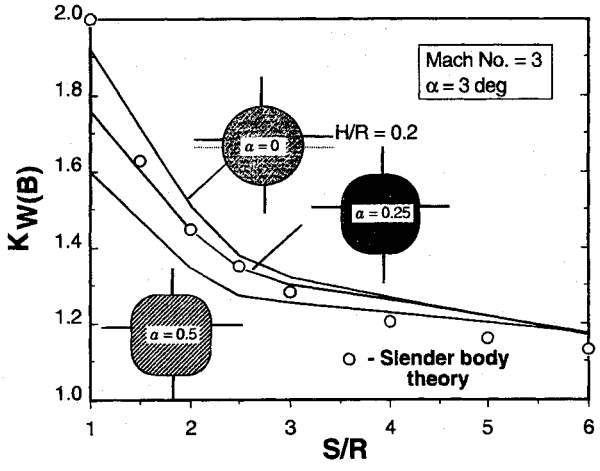

Fig. 11 Shape parameter effects on $K_{W(B)}$ for square cross sections as a function of S/R for wings located at $H/R = 0.2$.

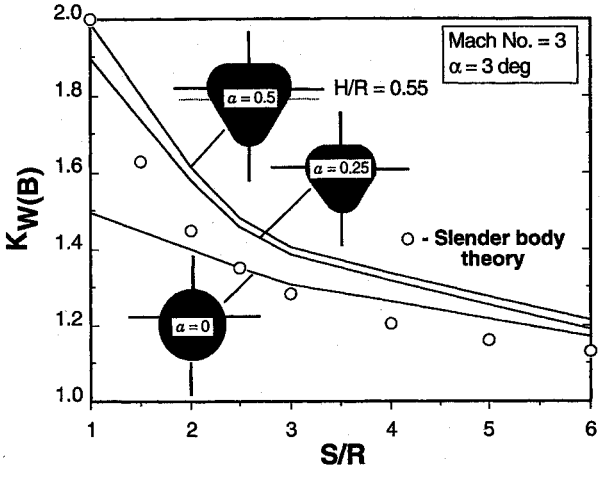

Fig. 12 Shape parameter effects on $K_{W(B)}$ for inverted triangular cross sections at S/R for wings located at $H/R = 0.550$, 0.425, and 0.300 for $a = 0.50$, 0.25, and 0.00, respectively.

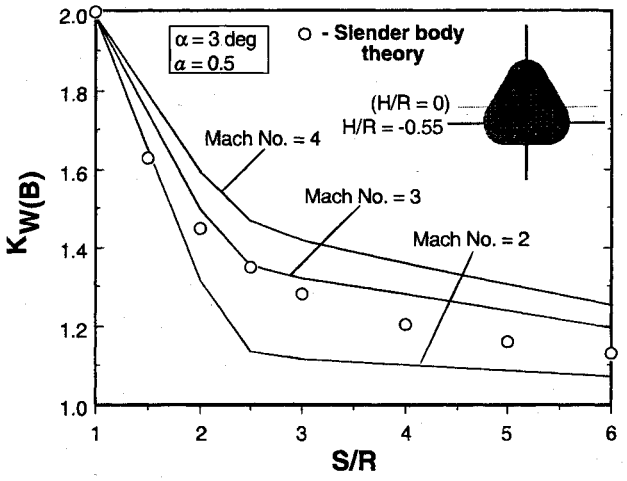

Fig. 13 Mach number effects on $K_{W(B)}$ for triangular cross sections with wings at $H/R = -0.55$ as a function of S/R.

velocities (upwash). The larger crossflow velocities magnify the wing–body interference and result in higher $K_{W(B)}$ values.

Mach Number Effects

Figure 13 shows the effects of Mach number and fin semispan on $K_{W(B)}$ for $a = 0.5$ triangles with wings located at $H/R = -0.55$. As Mach number increases, $K_{W(B)}$ increases for all S/R. This trend is evident for all cross-sectional shapes and wing H/R positions. Slender body theory $K_{W(B)}$ values are consistently lower than Euler $K_{W(B)}$ values Mach 3, but are consistently higher than Mach 2 values.

Tables 3, 4, 5, and 6 contain tabulated $K_{W(B)}$ data. The data presented here can be used for comparison of analytical, experimental, or theoretical results. Upon experimental validation, the tabulated Euler $K_{W(B)}$ results could be incorporated into an aeroprediction code as a table look-up routine for noncircular body engineering-level predictions to supplement slender body theory circular body $K_{W(B)}$ values.

Conclusions and Recommendations

The parametric effects of changing wing vertical position, Mach number, and body cross-sectional shape, on $K_{W(B)}$ have been investigated for supersonic body–wing missiles with noncircular fuselage cross sections. A spatial marching Euler code ZEUS has been used to compute the wing normal force in the presence of the body. Lifting surface theory has been used to compute wing-alone normal force for delta-wings. The results have been presented in terms of the component buildup parameter $K_{W(B)}$ for use in missile preliminary design. $K_{W(B)}$ exhibits sensitivity to changing wing vertical position, Mach number, and cross-sectional shape.

The effect of wing vertical positions above and below the missile centerline are favorable (increased $K_{W(B)}$ for square and triangular body missiles (flat windward facets), but adverse (decreased $K_{W(B)}$ for inverted triangular and circular cross-sectional shapes. The effect of increasing Mach number on $K_{W(B)}$ was favorable for all body cross-sectional shapes. The effect of increasing a on $K_{W(B)}$ was favorable for the inverted triangular bodies, but adverse for the triangular and square body cross sections.

It is recommended that wind-tunnel testing be performed to investigate the high angle of attack and sideslip behavior of noncircular missiles. The fuselage corners that generate the increased normal force in the pitch plane may cause unsymmetric vortex shedding when the missile is subjected to sideslip. The resulting induced forces and moments may be severe. Testing at full-scale Reynolds numbers would clarify the significance of these viscous effects.

Table 3 $K_{W(B)}$ values for circular fuselage cross sections

			S/R							
M	a	$\Delta H/R$	1	1.5	2	2.5	3	4	5	6
3	0.0	0.4	1.680	1.393	1.363	1.332	1.300	1.245	1.201	1.167
3	0.0	0.2	1.920	1.494	1.432	1.378	1.332	1.262	1.210	1.170
3	0.0	0.0	2.000	1.530	1.450	1.387	1.337	1.262	1.209	1.169
3	0.0	−0.2	1.920	1.499	1.419	1.361	1.316	1.246	1.198	1.161
3	0.0	−0.4	1.680	1.419	1.354	1.309	1.274	1.220	1.180	1.149

Table 4 $K_{W(B)}$ values for square fuselage cross sections

			S/R							
M	a	$\Delta H/R$	1	1.5	2	2.5	3	4	5	6
3	0.5	0.4	1.630	1.364	1.309	1.281	1.258	1.222	1.190	1.165
3	0.5	0.2	1.600	1.294	1.288	1.280	1.267	1.234	1.202	1.171
3	0.5	0.0	1.530	1.322	1.300	1.283	1.265	1.233	1.203	1.174
3	0.5	−0.2	1.600	1.416	1.343	1.299	1.270	1.226	1.193	1.166
3	0.5	−0.4	1.630	1.502	1.404	1.333	1.282	1.220	1.183	1.157
2	0.5	0.4	1.630	1.219	1.172	1.157	1.143	1.124	1.105	1.084
2	0.5	0.2	1.600	1.248	1.194	1.175	1.163	1.135	1.109	1.083
2	0.5	0.0	1.530	1.253	1.191	1.174	1.165	1.136	1.106	1.079
2	0.5	−0.2	1.600	1.240	1.172	1.153	1.142	1.117	1.093	1.069
2	0.5	−0.4	1.630	1.237	1.146	1.118	1.104	1.092	1.076	1.058
4	0.5	0.4	1.630	1.415	1.366	1.330	1.301	1.257	1.223	1.195
4	0.5	0.2	1.600	1.278	1.281	1.279	1.272	1.248	1.222	1.200
4	0.5	0.0	1.530	1.331	1.323	1.308	1.289	1.254	1.225	1.200
4	0.5	−0.2	1.600	1.474	1.421	1.371	1.331	1.271	1.230	1.200
4	0.5	−0.4	1.630	1.598	1.506	1.437	1.380	1.291	1.236	1.198

Table 5 $K_{W(B)}$ values for triangular fuselage cross sections

			S/R							
M	a	$\Delta H/R$	1	1.5	2	2.5	3	4	5	6
3	0.0	0.0	1.500	1.496	1.433	1.378	1.332	1.262	1.209	1.170
3	0.5	0.0	1.680	1.190	1.271	1.294	1.291	1.260	1.221	1.188
3	0.5	−0.2	1.990	1.403	1.393	1.368	1.339	1.284	1.236	1.197
3	0.5	−0.4	1.800	1.440	1.404	1.376	1.346	1.289	1.240	1.201
2	0.5	0.0	1.680	1.022	1.055	1.078	1.082	1.093	1.081	1.069
2	0.5	−0.2	1.990	1.195	1.144	1.129	1.116	1.108	1.090	1.072
2	0.5	−0.4	1.800	1.242	1.165	1.147	1.137	1.117	1.097	1.077
4	0.5	0.0	1.680	1.271	1.362	1.377	1.367	1.323	1.278	1.239
4	0.5	−0.2	1.990	1.543	1.521	1.478	1.434	1.356	1.297	1.252
4	0.5	−0.4	1.800	1.597	1.542	1.486	1.437	1.356	1.297	1.252

Table 6 $K_{W(B)}$ values for inverted triangular fuselage cross sections

			S/R							
M	a	$\Delta H/R$	1	1.5	2	2.5	3	4	5	6
3	0.0	0.0	1.500	1.496	1.433	1.378	1.332	1.262	1.209	1.170
3	0.5	0.4	1.98	1.687	1.571	1.488	1.421	1.327	1.263	1.215
3	0.5	0.2	1.99	1.644	1.554	1.478	1.415	1.325	1.260	1.215
3	0.5	0.0	1.68	1.350	1.407	1.395	1.364	1.302	1.245	1.207
2	0.5	0.4	1.98	1.506	1.366	1.302	1.259	1.190	1.145	1.118
2	0.5	0.2	1.99	1.416	1.323	1.270	1.230	1.180	1.144	1.116
2	0.5	0.0	1.68	1.188	1.211	1.206	1.186	1.165	1.135	1.114
4	0.5	0.2	1.99	0.859	1.087	1.193	1.242	1.264	1.251	1.227
4	0.5	0.0	1.68	1.347	1.422	1.416	1.395	1.340	1.289	1.247

Appendix A: Development of the Shape Parameter a

Parameter a quantifies the cross-sectional shape of the missile fuselage. At $a = 0$, the shape is circular, and at $a = 1$, the shape is sharp cornered; i.e., a sharp cornered square. Figure 14 shows the relationship between shape factor and the geometry of the noncircular fuselage cross sections. For the square cross sections, the circular fillet, defined by R_f, is scribed over an arc of 90 deg. For the triangular cross sections, R_f is scribed over a 120 deg arc. For the circular cross section, the fillet scribes a circle. R_f and a' are defined in terms of the radius R of the inscribed circle (Fig. 14)

$$R = R_f + a' \tag{A1}$$

Thus we can write,

$$a'/R + R_f/R = 1 \tag{A2}$$

However, the parameter a is defined as a'/R so that

$$a = 1 - R_f/R \tag{A3}$$

As a approaches 0, R_f approaches R, and as a approaches 1, R_f approaches 0. For all shapes R was 1.0-cm, implying that all fuselage shapes collapse to an identical, circular cross section.

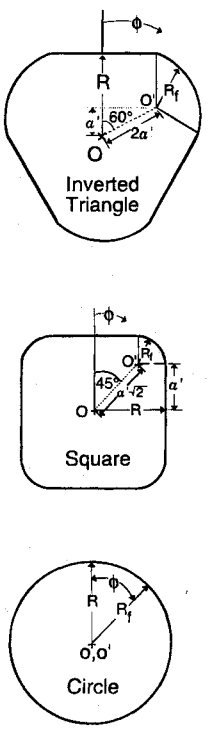

Fig. 14 Shape parameter geometry.

Acknowledgments

This work has been supported by McDonnell Douglas Missile Systems Company (MDMSC) of St. Louis, Missouri through the Independent Research and Development Program, monitored by Kurt Bausch and Andrew Jenn. Additional funds were provided by the Missouri Research Assistance Act. The authors appreciate and acknowledge the constructive comments of the reviewers.

References

[1] Est, B. E., "Computational Aerodynamics of Supersonic Missiles with Noncircular Fuselage Cross Section," M.S. Thesis, Department of Mechanical and Aerospace Engineering, Univ. of Missouri—Rolla, Rolla, MO, May 1991.

[2] Carlson, H. W., and Gapcynski, J. P., "An Experimental Investigation At a Mach Number of 2.01 of the Effects of Body Cross-Section Shape On the Aerodynamic Characteristics of Bodies and Wing-Body Combinations," NACA RM L55E23, July 1955.

[3] Jorgensen, L. H., "Inclined Bodies of Various Cross Sections at Supersonic Speeds," NASA Memo 10-3-58A, Nov. 1958.

[4] Sigal, A., "Methods of Analysis and Experiments for Missiles With Noncircular Fuselages," *Tactical Missile Aerodynamics: Prediction Methodology*, edited by M. R. Mendenhall, Vol. 142, Progress in Aeronautics and Astronautics Series, AIAA, Washington, DC, 1991, pp. 171–224.

[5] Est, B. E., and Nelson, H. F., "Supersonic Aerodynamics of Noncircular Cross Section Missile Forebodies," *Journal of Aircraft*, Vol. 29, No. 4, 1992, pp. 612–618.

[6] Est, B. E., and Nelson, H. F., "Wing–Body Carryover and Fin Center of Pressure for Missiles with Noncircular Fuselages," AIAA Paper 91-2856, Aug. 1991.

[7] Est, B. E., and Nelson, H. F., "Fin Dihedral Effects on Aerodynamics of Supersonic Missiles with Square and Triangular Fuselage Cross Sections," AIAA Paper 91-3256, Sept. 1991.

[8] Pitts, W. C., Nielsen, J. N., and Kaatari, G. E., "Lift and Center of Pressure of Wing–Body–Tail Combinations at Subsonic, Transonic, and Supersonic Speeds," NACA Rep. 1307, July 1953.

[9] Nielsen, J. N., *Missile Aerodynamics*, McGraw-Hill, 1960; also, republished by Nielsen Engineering and Research, Inc., Mountain View, CA, 1988.

[10] Hemsch, M. J., "Component Build-Up Method for Engineering Analysis of Missiles at Low-to-High Angles of Attack," *Tactical Missile Aerodynamics: Prediction Methodology*, edited by M. R. Mendenhall, Vol. 142, Progress in Aeronautics and Astronautics Series, AIAA, Washington, DC, 1991, pp. 115–169.

[11] Vukelich, S. R., and Jenkins, J. E., "Evaluation of Component Build-up Methods for Missile Aerodynamic Predictions," *Journal of Spacecraft and Rockets*, Vol. 19, No. 6, 1983, pp. 481–488.

[12] Krieger, R. J., and Williams, J. E., "Accuracy Criteria for Evaluating Supersonic Missile Aerodynamic Coefficient Prediction," *Journal of Spacecraft and Rockets*, Vol. 20, No. 4, 1983, pp. 323–330.

[13] Stoy, S. L., and Vukelich, S. R., "Prediction of Aerodynamic Characteristics of Unconventional Missile Configurations Using Component Buildup Technique," AIAA Paper 86-0489, Jan. 1986.

[14] Bruns, K. D., Moore, M. E., Stoy, S. L., Vukelich, S. R., and Blake, W. B., "Missile Datcom, User's Manual—Rev. 4/91," Air Force Wright Aeronautical Laboratories, Wright-Patterson AFB, OH, WL-TR-91-3039, April 1991.

[15] Devan, L., "Aerodynamics of Tactical Weapons to Mach Number 8 and Angle of Attack 180°: Part I, Theory and Application," Naval Surface Weapons Center, Dahlgren, VA, NSWC TR-80-346, Oct. 1980.

[16] Lesieutre, D. J., Mendenhall, M. R., Nazario, S. M., and Hemsch, M. J., "Prediction of the Aerodynamic Characteristics of Cruciform Missiles Including Effects of Roll Angle and Control Deflection," Nielson Engineering and Research, Mountain View, CA, NEAR TR-360, Aug. 1986.

[17] Wardlaw, A. B., Jr., and Davis, S. F., "A Second-Order Godunov Method for Tactical Missiles," Naval Surface Weapons Center, Dahlgren, VA, NSWC-TR 86-506, Dec. 1986.

[18] Wardlaw, A. B., Jr., and Priolo, F. J., "Applying the ZEUS Code," Naval Surface Weapons Center, Dahlgren, VA, NSWC-TR 86-508, Dec. 1986.

[19] Wardlaw, A. B., Jr., Baltakis, F. P., Martin, F. M., Priolo, F. J., and Jettmar, R. U., "A Godunov Method for Supersonic Tactical Missiles," *Journal of Spacecraft and Rockets*, Vol. 24, No. 1, 1987, pp. 40–47.

[20] Polhamus, E. C., Geller, E. W., and Grunwald, K. J., "Pressure and Force Characteristics of Noncircular Cylinders as Affected by Reynolds Number With a Method Included for Determining the Potential Flow About Arbitrary Shapes," NASA TR R-46, March 1959.

[21] Jenn, A. A., and Nelson, H. F., "Wing Vertical Position Effects on Lift for Supersonic Delta Wing Missiles," *Journal of Spacecraft and Rockets*, Vol. 26, No. 4, 1989, pp. 210–216.